Semi-Linear Induction Motor

Edgar Ramos and Jacob Vangunten

Project Advisor: Professor Steven D. Gutschlag

Bradley University Department of Electrical Engineering

May 12, 2016

I. Abstract

A Linear Induction Motor (LIM) is a specific type of alternating current (AC), multiple-phase machine that provides force and movement in a linear direction. Numerous applications of LIM's can be found in industry today, one of the most interesting being high speed magnetic levitation railway systems. The fundamental goal of this project is to determine the reasons for the limited functionality of the previous team's SLIM design. The current SLIM is using a rotor that was used for a magnetic levitation senior project. It is suspected that the problem with the existing rotor is that it has no ferromagnetic material beneath the conducting bars to increase the flux density in the air gap between the stator and the rotor. Therefore, a new rotor was designed with a better magnetic circuit for this application.

Table of Contents

I. Introduction

A. Project Background

A linear induction motor (LIM) is a specific type of alternating current (AC) machine designed to produce motion in a straight line. A LIM operates under the same principles as its AC rotary motor counterpart, typically powered by a three-phase voltage source with a force that is produced by a moving magnetic field. The main difference between a typical rotary motor and a LIM is the way the magnetic field is produced. Inside of an AC rotary motor the magnetic field produced travels in a continuous rotary motion. A LIM can be imagined as an AC rotary motor cut down the center and the stator and rotor spread out along a flat line. The induced magnetic field now moves linearly across the flat motor face instead of rotating. A semi-linear induction motor is similar to the linear induction motor with the exception that the stator is not completely flat. The force created by the SLIM magnetic field can be used to drive large diameter rotors.

B. Project Statement

The initial project goal is to understand reasons for the limited functionality of the 2016 Semi-Linear Induction Motor design. The 2016 SLIM design included a rotor that was used for a magnetic levitation senior project completed several years ago. It is suspected that the fundamental problem with the current rotor is that it has no ferromagnetic material to increase the flux density in the air gap. Therefore, the primary project goal is to design, construct, and test a new rotor that will provide a better magnetic circuit to increase the developed rotor torque. The SLIM will be thoroughly tested and modified until reasonable functionality is attained. The SLIM will use the stator that was developed by the 2016 team. All functional requirements will also be met.

II. Prior Work

The goals of the 2016 SLIM project team included designing and building a stator that could be mounted under a 45.72cm diameter wheel used in a previous senior project to induce wheel rotation. The main focus of the project was to design and implement a SLIM that could eventually be used to power and control a magnetic levitation system for future senior design projects. Their design objectives included the use of inexpensive materials, electrical efficiency, controllability, safe operation, easily constructible, and reliable operation. The 2016 LIM team developed the design equations needed for their stator design, and had the stator constructed with steel laminations. Additionally, the team wound coils that had four layers with 235 turns each, and placed a coil on each of

the twelve stator teeth. The coils were then secured with cloth tape and zip ties. Furthermore, the project team designed a base to mount the rotor, and wired the coils in a three-phase wye configuration. Unfortunately, budget constraints prevented the team from incorporating a new rotor design. Therefore, the 2016 SLIM design which resulted in very limited available rotational torque. Hence, the SLIM was only able to spin the rotor very slowly, and required a small externally applied manual torque to initiate rotation.

III. Standards and Patents Applicable to the Project

- G. A. Francis. “Linear induction motor construction.” U.S. Patent 3155851 A, Nov. 3, 1964.
- T. Fellows, E.Laithwaite. “Secondary member for single-Sided linear induction motor.” U.S. Patent 3824414 A, Mar.13, 1973.
- N. B. John. “Linear induction motor.” U.S. Patent 3628072 A, Jun. 17, 1970.

IV. Subsystem Level Functional Requirements

A. Functional Requirements: Subsystem Level

A three-phase, 208[Vrms] AC source powered the Lenze AC Tech (model MH250B) Variable Frequency Drive (VFD). The VFD was used to vary the frequency and voltage provided to the SLIM stator coils to produce a moving magnetic field along the length of the stator. The moving magnetic field induced a force along the periphery of the rotor, thereby generating a torque about the axis of rotation.

As indicated in the Project Statement section above, the primary project goal was to design, construct, and test a new rotor that would provide a better magnetic circuit to increase the developed rotor torque. Although the VFD factory default setting is to operate over a frequency range of 0 – 60[Hz], the frequency range can be modified via the “Base Freq” parameter available in the Lenze AC Tech programming menu to a maximum of 360[Hz]. The 2016 LIM project team designed the stator to operate at 120[Hz], but never altered the “Base Freq” parameter to implement the change.

1. Variable Frequency Drive Subsystem

- Display
  - Desired output frequency
  - Actual VFD output frequency
  - Percent of maximum designed load current for existing operating condition
  - Operating fault condition indicator

B. Subsystem Block Diagram

As indicated above, the SLIM was powered and controlled by a model MH250B Lenze AC Tech Variable Frequency Drive (VFD). Figure 1 below provides a block diagram to illustrate the various subsystems included in the SLIM system.

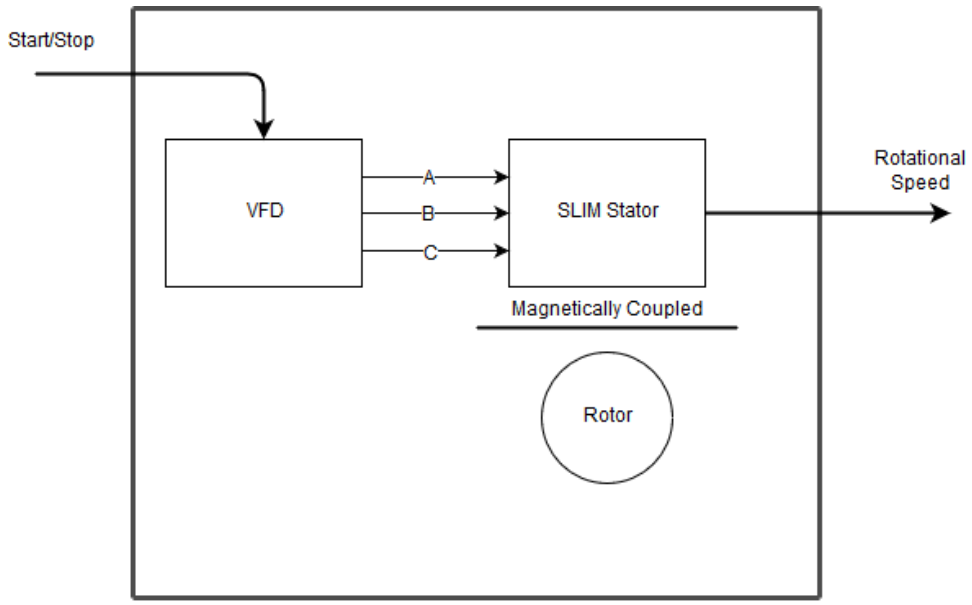

Fig. 1 Subsystem block diagram illustrating various subsystems and connections.

C. Engineering Efforts

The initial goal was to troubleshoot the previous SLIM project team's design, and thoroughly test the SLIM in an attempt to determine the reasons for its poor performance. Significant effort was dedicated to analyzing the previous team's design equations to uncover possible errors, but found no serious problems with the design. After thoroughly reviewing the previous team's design equations, experiments were undertaken to uncover possible electrical connection errors in the experimental SLIM apparatus.

A DC current of 1.5 [A] was applied to each coil. The voltage required to attain the 1.5 [A] for each coil was measured to verify there were no short-circuits embedded in the coil windings and that no significant differences existed between the coil resistances. Fortunately, no short-circuits were discovered, and the required applied voltages were nearly identical for all coils at a current of 1.5[A].

The next step was to analyze the magnetic polarities associated with the current through each set of phase coils. As each set of phase coils was energized, a compass was used to obtain an approximate mapping of the magnetic field each phase was producing. The mapping indicated the various coils associated with each phase appeared to be connected correctly.

The 2016 SLIM project team had the system configured as a WYE connection. Although the system was originally designed to operate in a WYE configuration, the stator was wired in a DELTA configuration to obtain higher stator phase currents for short-duration operation. The DELTA configuration resulted in phase currents about three times those measured with the WYE connection, but the developed rotor torque was still minimal. The project advisor increased the VFD frequency to about 40[Hz], and it became obvious that the rotor was finally beginning to rotate without external assistance. To verify that the apparent effect was real, the rotor was pushed in the opposite direction by hand with the VFD frequency set at 40[Hz], and it was obvious a torque was present in the direction opposite to the pushing torque. Although, the SLIM was tested for short intervals connected in DELTA configuration, it was originally designed for a WYE configuration and will be operated as such. However, it was noted during the rotor design process that it was also theoretically possible that the redesigned rotor could increase the inductance of the combined stator and rotor magnetic circuit, so the effective coil impedance would increase significantly. Although that was ultimately found to be the case, no-load three-phase DELTA connection tests indicated the stator phase currents were at the designed phase coil current limit. In addition, since smaller currents may be sufficient to generate the torque required to turn the rotor at the desired speed and load, the team plans to leave the system connected in a WYE configuration.

D. Parts List

Table I: Parts List

Component	Method of Procuring	Cost if Applicable
Rotor shaft	Used Existing	N/A
Bearings	Used Existing	N/A
Manufactured Rotor	Purchasing	$575
Copper or aluminum bars	Used Existing	N/A
Various bolts, screws, and nuts	Used Machine Shop Supply	N/A

E. Division of Labor

Table II: Division of Labor

Tasks	Group Members
Review and Analyze Design Equations	Edgar and Jacob
Determine Coil Orientation	Edgar and Jacob
Test for Short-circuits	Edgar and Jacob
Map the Magnetic Field	Edgar and Jacob
Configure and Test Delta Connection	Edgar and Jacob
Research and Design New Rotor	Edgar and Jacob

V. Design and Solution

A. Initial Design Approach

The main goal of this capstone project was to increase the efficiency of the 2016 team's Semi-Linear Induction Motor project. The SLIM consists mainly of a stator and a rotor. Last year's team designed a stator for the motor which resulted in very minimal rotational torque on the existing polymer rotor. The 2017 SLIM team had several options relative to the design and construction of a new rotor. After running a variety of tests it was

determined that the existing rotor was not receiving enough flux. For that reason the new rotor design would need to be constructed with laminated electrical sheet steel. One option investigated was to design the rotor with a lightweight aluminum center surrounded with sheet steel laminations on the outer periphery. The other option discussed was to fabricate the entire rotor with sheet steel laminations.

It was determined that the primary disadvantage of using an aluminum center with a sheet steel periphery was the problem of securely attaching the sheet steel laminations to the aluminum center without significantly disturbing the rotational balance of the structure. It should be noted that the 2016 SLIM team had difficulty balancing a one-piece solid polymer rotor used in the first design, and therefore attempting to balance a two-piece structure seemed to be a very significant and costly risk. It was ultimately determined that the better option would be the one-piece sheet steel rotor with as much material removed from the center portion of the structure as possible. The main disadvantage of a one-piece sheet steel rotor is the weight. Even with as much material removed from the center portion as structural stability permits, calculations estimated that the design would weigh about 43 pounds.

The majority of the team's lab time was used to analyze the 2016 SLIM team's stator design, develop equations for the magnetic structure's inductance, obtain experimental data to verify the inductance equations, and design the new rotor.

The size of the new rotor needed to be similar to the existing unit so that existing parts such as the SLIM stator, rotor shaft, copper track, and support structure could still be used. Laser Laminations was selected to build the sheet steel rotor because of the excellent quality of the stator they manufactured for the 2016 SLIM team. Although numerous versions were considered and reviewed by the staff at Laser Laminations, Figure 4 below provides a view of the final rotor design.

B. Equation Implementation

The first steps in the design of the rotor were to theoretically determine the inductance for the SLIM magnetic structure for three different types of rotors. The first model was a polymer rotor (magnetic permeability essentially the same as air) with thin steel sheets around the periphery. The second model was a rotor made of polymer without any steel sheets around the periphery, so the entire structure had the same permeability as air. The third rotor model was a steel rotor with a magnetic path 0.75 [in] thick and 2 [in] wide designed by the 2017 SLIM design team. Equation (1.1) can be used to estimate the theoretical inductance of two coils.

$$L = \frac{\lambda}{I_L} = \frac{N\Phi}{I_L} \tag{1.1}$$

where L is inductance, λ is the total flux linkage, I_L is the inductor current, and N is the number of turns. Equation (1.1) can be modified to obtain Equation (1.2),

$$\Phi = \frac{\mathcal{F}}{\Re_{Tot}} = \frac{NI_L}{\Re_{Tot}} \tag{1.2}$$

where Φ is the flux, $\mathcal{F}$ is magnetomotive force, and $\Re_{Tot}$ is the total reluctance. The total reluctance is then Equation (1.3),

$$\Re_{Tot} = \Re_{p1} + \Re_{p2} + \Re_{ag1} + \Re_{ag2} + \Re_{rotor} + \Re_B \tag{1.3}$$

where $\Re_{p1}$ and $\Re_{p2}$ are the reluctance of the poles, $\Re_{ag1}$ and $\Re_{ag2}$ are the reluctance of the air gaps, $\Re_{rotor}$ is the reluctance of the rotor, and $\Re_B$ is the reluctance of the base or stator. The reluctance of the poles, air gaps, rotor, and stator are Equations (1.4), (1.5), (1.6), and (1.7) respectively.

$$\Re_{p1} = \Re_{p2} = \frac{l_p}{\mu_r \mu_o A_p} \tag{1.4}$$

$$\Re_{ag1} = \Re_{ag2} = \frac{l_{ag}}{\mu_o A_{ag}} \tag{1.5}$$

$$\Re_{rotor} = \frac{l_{rotor}}{\mu_o \mu_r A_{rotor}} \tag{1.6}$$

$$\Re_B = \frac{l_B}{\mu_r \mu_o A_B} \tag{1.7}$$

Where A_p is the cross-sectional area of the poles, A_{ag} is the cross-sectional area of the air gaps, A_{rotor} is the cross-sectional area of the rotor, A_B is the cross-sectional area of the stator, l_p is the pole length, l_{ag} is the length of the air gap, l_{rotor} is the rotor length, l_B is the stator length, μ_r is the relative permeability, and μ_o is the permeability of free space. Substituting Equations (1.4), (1.5), (1.6), (1.7) into Equation (1.3) yields Equation (1.8) shown below.

$$\Re_{Tot} = \frac{l_{p1}}{\mu_r \mu_o A_{p1}} + \frac{l_{p2}}{\mu_r \mu_o A_{p2}} + \frac{l_{ag1}}{\mu_o A_{ag1}} + \frac{l_{ag2}}{\mu_o A_{ag2}} + \frac{l_{rotor}}{\mu_r \mu_o A_{rotor}} + \frac{l_B}{\mu_r \mu_o A_B} \quad (1.8)$$

Equation (1.8) can be substituted into Equation (1.2) to yield Equation (1.9) shown below.

$$\Phi = \frac{NI_L}{\frac{l_{p1}}{\mu_r \mu_o A_{p1}} + \frac{l_{p2}}{\mu_r \mu_o A_{p2}} + \frac{l_{ag1}}{\mu_o A_{ag1}} + \frac{l_{ag2}}{\mu_o A_{ag2}} + \frac{l_{rotor}}{\mu_r \mu_o A_{rotor}} + \frac{l_B}{\mu_r \mu_o A_B}} \quad (1.9)$$

Substitution of Equation (1.9) into equation Equation (1.1), and rearranging yields Equation (1.10).

$$L = \frac{N(\mu_r \mu_o A_{p1} A_{p2} A_{ag1} A_{ag2} A_{rotor} A_B)}{2l_p A_{rotor} A_{ag} A_B + 2l_{ag} A_{rotor} A_p A_B \mu_r + l_{rotor} A_p A_{ag} A_B + l_B A_p A_{ag} A_{rotor}} \quad (1.10)$$

After developing the theoretical analysis of the combined stator/rotor inductance the circuit shown in Figure 2 was designed to determine the polarity of the poles.

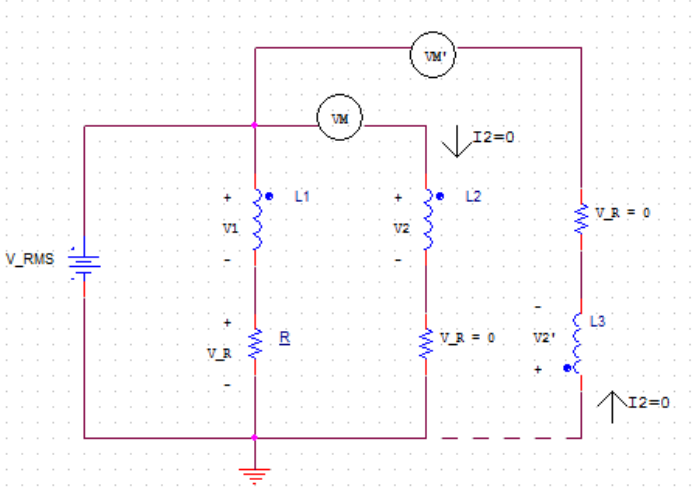

Fig. 2. Circuit to Determine Coil Orientation

The source voltage is V_{RMS}, the primary coil voltage is V_1, the resistor voltage is V_2, the inductance voltage is $V_L = V_1 + V_R$, the coil current is I, the secondary coil voltage is V_2, the voltmeter voltage is VM, the inverted secondary coil voltage is V_2', and the flipped voltmeter voltage is VM'. The measurements made involved all of the previously stated parameters for 100Hz and 500Hz without a rotor in place and then with a steel bar across the north and south pole at 500 Hz. Once the data was taken, Equation (1.11) was

developed from the circuit in Figure 3 to determine the measured inductance. Note that the resistance of the coils was only 0.52[Ω], and was neglected in Equation (1.11)

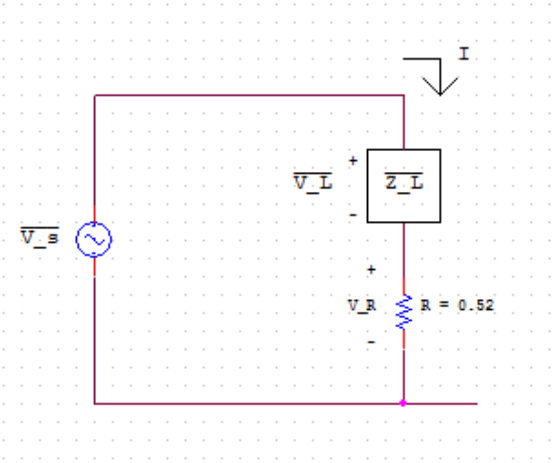

Fig. 3. Circuit used for Calculating Measured Inductance

$$\overline{V_L} = \bar{I} * \overline{Z_L} \Rightarrow \overline{Z_L} = \frac{\overline{V_L}}{I} \Rightarrow |\overline{Z_L}| = \frac{V_L}{I} \Rightarrow 2\pi f L = \frac{V_L}{I} \Rightarrow L = \frac{V_L}{I(2\pi f)} \quad (1.11)$$

Furthermore, the following equations show the relationship between output power and phase inductance. As shown in Equation (1.17), the greater the phase inductance, the greater the output power. From Equation (1.17), it was determined that the new rotor design would increase the inductance, which would then increase the output power.

$$P_{out} = 6.66 * P * f_m * \Phi_{ag} * T_{ph} * K_w * I_{ph} * \eta * (P.F.) \quad (1.12)$$

$$P_{out} = 6.66 * P * f_m * \lambda_{ph} * K_w * I_{ph} * \eta * (P.F.) \quad (1.13)$$

$$\lambda_{ph} = T_{ph} * \Phi_{ag} \quad (1.14)$$

$$P_{out} = 6.66 * P * f_m * \frac{\lambda_{ph}}{I_{ph}} * K_w * I_{ph}^2 * \eta * (P.F.) \quad (1.15)$$

$$P_{out} = 6.66 * P * f_m * L_{ph} * K_w * I_{ph}^2 * \eta * (P.F.) \quad (1.16)$$

$$P_{out} = K * L_{ph} \quad (1.17)$$

$$\textit{Where: } K = 6.66 * P * f_m * K_w * I_{ph}^2 * \eta * (P.F.) \quad (1.18)$$

where P is the number of poles, f_m is the mechanical frequency, Φ_{ag} the air gap flux, T_{ph} is the turns per phase, K_w is constant, I_{ph} is the current per phase, η is the efficiency, and $P.F.$ is the power factor.

C. Final Design

The final design of the SLIM rotor is a 17.93 [in] diameter-wheel fabricated from welded sheet steel laminations. There is a 60 degree angle between each of the six rotor spokes. As shown in the figure 3 above, the rotor was designed with a 0.5 [in] radius where the spokes met the periphery of the structure, and a 2 [in] radius where two spokes met at the hub of the structure. The addition of the various radii increased the structural integrity of the overall rotor. The inner diameter was selected to be 16.75 [in] to provide an adequate magnetic flux path around the periphery of the rotor without adding more weight than was necessary. The design of the rotor included 1 [in] hole with a ¼ [in] keyway so the previous rotor's shaft could be re-used. After the rotor design was finalized, it only took about 10 days to receive the fabricated rotor from Laser Laminations.

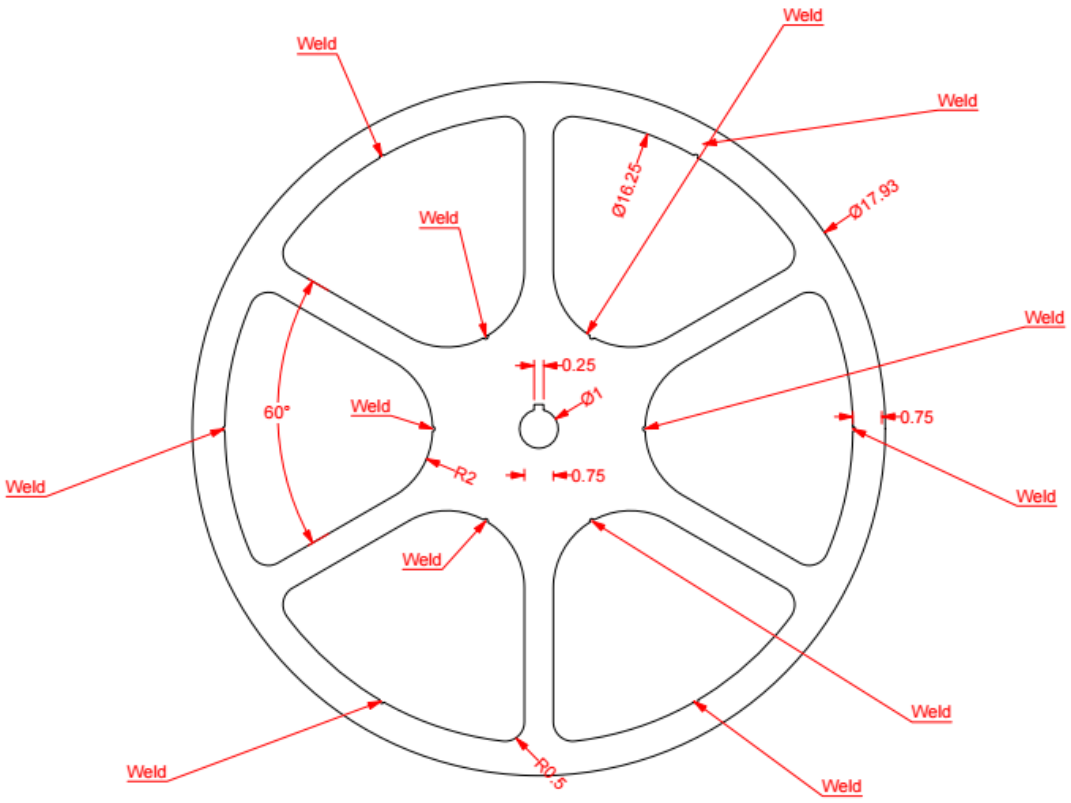

Figure 4. Final Iteration for the New Rotor Design

A. SLIM Testing

During the process of attempting to test the new rotor, the VFD was detecting faults and shutting down. After examining the coils and running some tests, it was found that two coils were shorting out to the stator. After the two coils were taken off the stator and repaired, the SLIM was able to function without generating VFD faults.

The testing of the SLIM started with taking air gap measurements at the 1st A coil on the left of the stator, the 2nd C coil and 3rd A coil at the bottom of the stator, and the 4th C coil on the left of the stator. The air gaps, including the copper track, were 0.183 [in], 0.185 [in], and 0.17 [in] respectively. Next, during the tests the voltage across each phase, the current through phase B, the VFD percentage load, and the rotor speed were recorded. After initial tests it was found that the copper track was heating up and expanding due to the fact that not all of the screw locations around the track were used, leaving small air gaps that prevented adequate heat transfer from the copper track to the metal portion of the rotor. The copper track was then hitting the stator as it rotated, thus slowing the rotor down. To avoid this problem, the SLIM was permitted to cool down before running additional tests at different frequencies. The following table contains all of the data taken during the testing.

Table III: SLIM Test Data

Frequency	20 [Hz]	25 [Hz]	30 [Hz]	35 [Hz]	40 [Hz]	45 [Hz]	50 [Hz]	55 [Hz]	60 [Hz]
Phase A Voltage	60 [V]	69 [V]	75 [V]	81 [V]	89 [V]	96 [V]	104 [V]	112 [V]	121 [V]
Phase B Voltage	56 [V]	65 [V]	71 [V]	78 [V]	85 [V]	91 [V]	99 [V]	108 [V]	116 [V]
Phase C Voltage	60 [V]	70 [V]	76 [V]	83 [V]	90 [V]	99 [V]	107 [V]	116 [V]	124 [V]
Current	1.1 [A]	1.4 [A]	1.5 [A]	1.8 [A]	2 [A]	2 [A]	2.2 [A]	2.3 [A]	2.5 [A]
Speed	8.2 RPM	13.5 RPM	17 RPM	21 RPM	25.75 RPM	30 RPM	37 RPM	41 RPM	45 RPM
Load Percentage	11%	11 %	12 %	13 %	13 %	14 %	14 %	15 %	16 %

The next step in testing was to calculate the slip percentage at each frequency. The slip was calculated using Equation (1.19).

$$Slip = \frac{Synchronous\ speed - Measured\ speed}{Synchronous\ speed} \tag{1.19}$$

The Table IV contains the calculated slip for each operating frequency.

Table IV: Frequency vs. Slip Percentage

Frequency	Slip Percentage
20 [Hz]	94.5 %
25 [Hz]	92.8 %
30 [Hz]	92.44 %
35 [Hz]	92 %
40 [Hz]	91.4 %
45 [Hz]	91.1 %
50 [Hz]	90.1 %
55 [Hz]	90.06 %
60 [Hz]	90 %

VI. Project Timeline

The SLIM project for the fall semester was divided into review and analysis of design equations, determination of coil orientation, test for short-circuits, mapping of the magnetic field, configuration and testing of a delta connection, and researching and designing a new rotor. The time spent on reviewing and analyzing the previous team's design equations was from November 3rd to November 8th. The time from November 10th to November 15th was used to determine the correct coil orientations. November 15th to November 17th was dedicated to testing the SLIM to determine if any coil short-circuits were present, to map the stator magnetic field, and confirm the delta connection was correct. Between November 22nd to December 9th the project team researched and planned the design of the new rotor.

As indicated in the proposed schedule for the spring semester shown in Figure 5, tasks included designing and constructing the new rotor, mounting and testing the new rotor, thoroughly testing the system and making improvements. The design and construction of the new rotor was scheduled to take place from January 27th to February 7th. The mounting and testing of the new rotor was scheduled for February 9th to February 21st. Finally, the work on the final report and final presentation was scheduled for April 4th to May 2nd. Although the project timeline did not follow the exact schedule presented in Figure 5, the work was all completed by May 12, 2017.

Figure 5: Fall and Spring Schedule

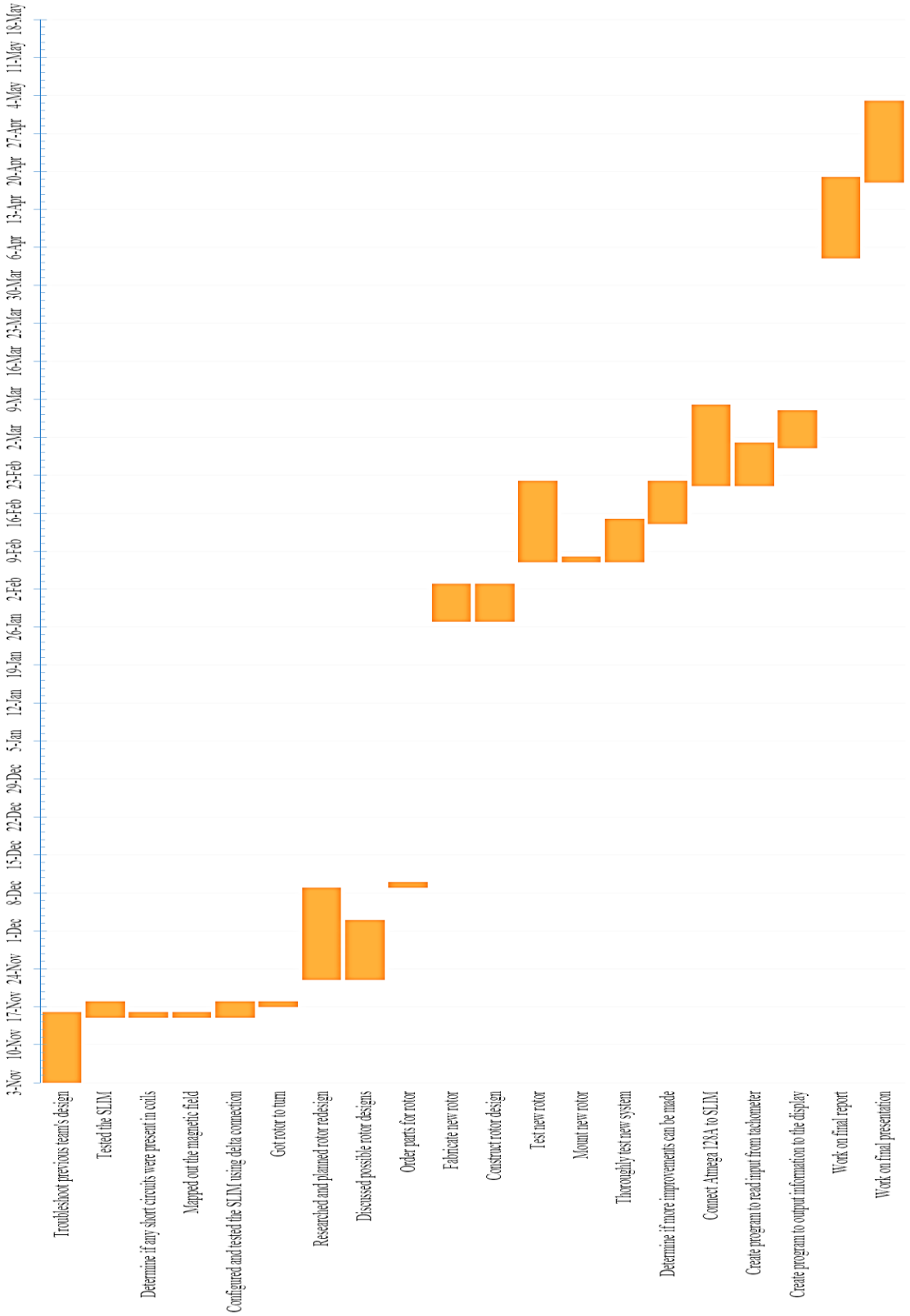

VII. Results and Conclusions

The results with the old rotor were unsatisfactory because the motor needed assistance in order for the rotor to move. The VFD was set to 60 Hz and required someone to push the rotor along to help it start to rotate, even though it was operating at maximum voltage at that frequency. In contrast, the new rotor design enabled the new rotor to rotate on its own starting at 20 Hz. Furthermore, the new rotor was operating better at 20 Hz than the old rotor did at 60 Hz. Prior to this the 2017 SLIM team had not seen any rotation at 20 Hz.

After performing the tests on the SLIM, recording the data, and calculating the slip, the data shows that the large amount of slip is causing the SLIM to function at lower speeds. The reason the slip is very high is because of the large air gap between the rotor and the stator. If the air gap was smaller, the slip would be reduced and permit the SLIM to run at higher speeds.

The previous SLIM team designed the stator coils to be easily removed from the stator core so the coils could be redesigned to obtain higher power output if deemed necessary in the future. The next iteration of the SLIM system as a senior project could conduct further testing to identify areas that could improve results. Furthermore, future teams could add a control scheme to the SLIM system. In addition, future teams could focus on combining the SLIM with a magnetic levitation system. Note, however, that the cost of such improvements may be significant because of the expensive components and manufacturing processes.

VIII. References

1. Subsystem Block Diagram. [Drawing]
2. Linear Induction Motor: 2016 Senior Design Project Team of Tyler Berchtold, Mason Biernat, and Tim Zastawny
3. Steven Gutschlag, Project Advisor

IX. Appendix A

Figures

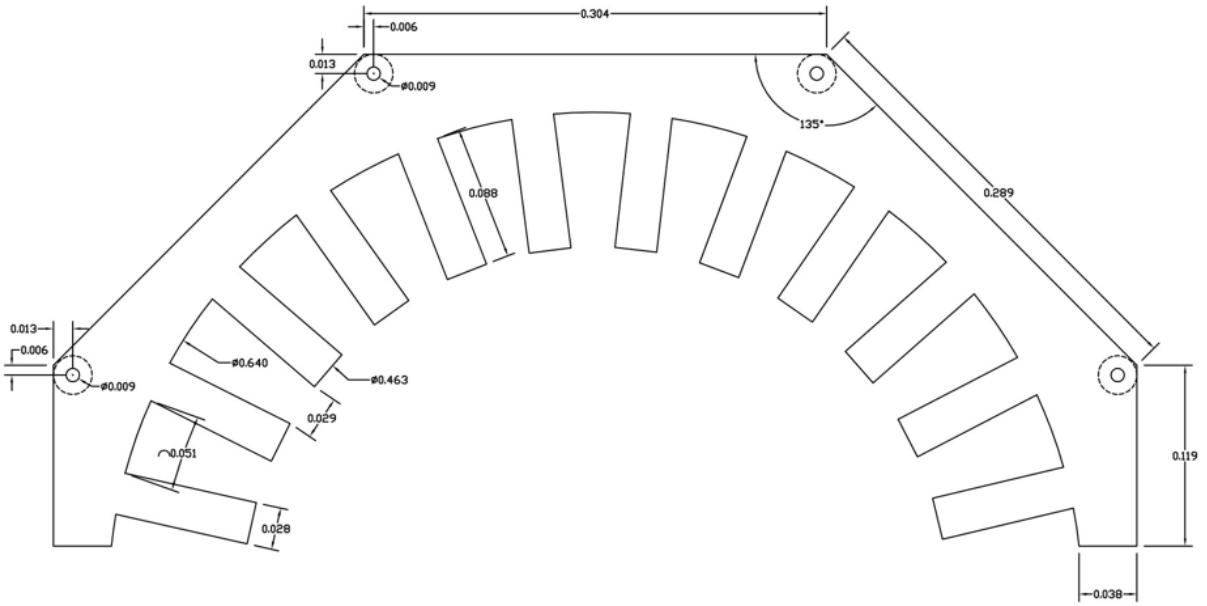

Fig. 6 Stator design developed from previous project team

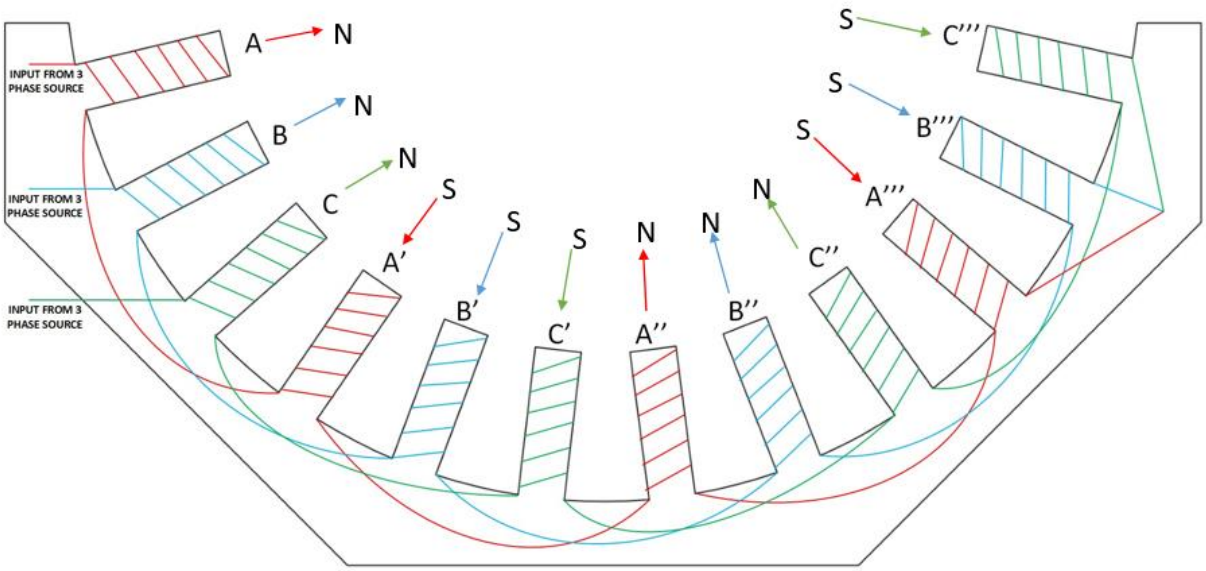

Fig. 7 Illustration of the stator wiring

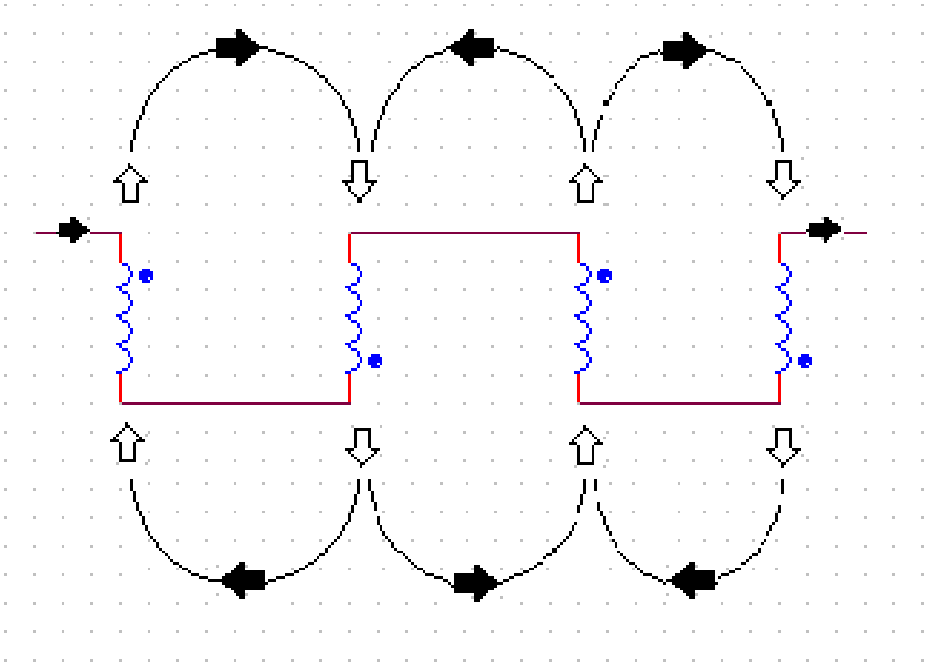

Fig. 8 Coil Orientation and Magnetic Field for One Phase

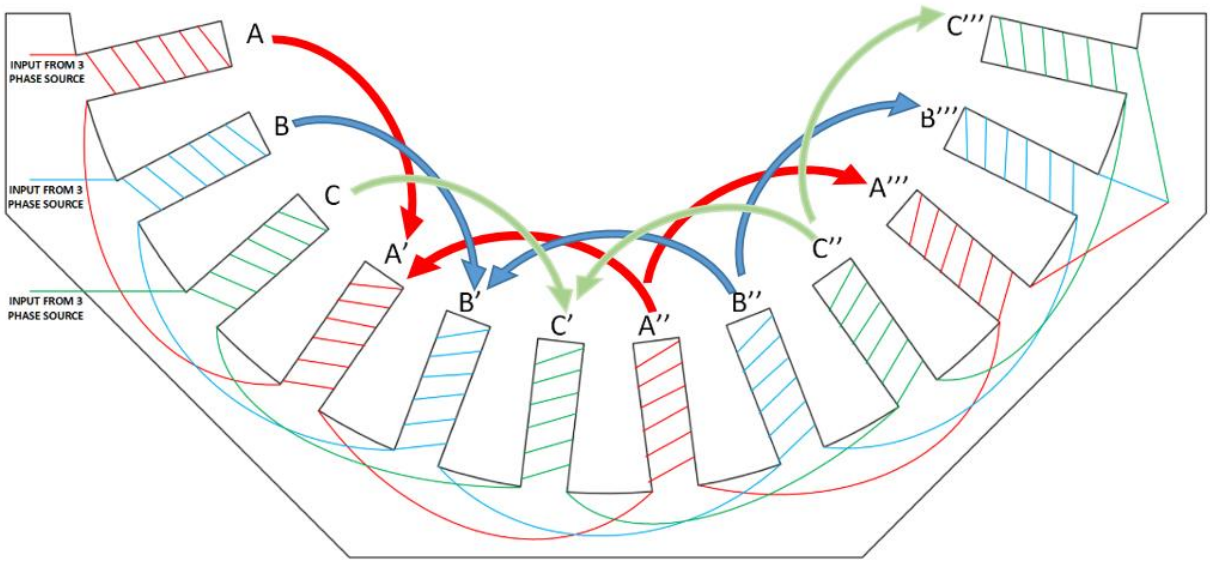

Fig. 9 Magnetic Field Mapping

Citations used for Figures in Appendix A

[1] Stator Design. [Diagram]. Retrieved from 2016 LIM Senior Electrical Engineering Project Final Report.
[2] Stator Wiring Diagram. [Diagram]. Retrieved from 2016 LIM Senior Electrical Engineering Project Final Report.